

# Two-dimensional Simulation of All-solid-state Lithium-ion Batteries

Lizhu Tong

Keisoku Engineering System Co., Ltd.

1-9-5 Uchikanda, Chiyoda-ku, Tokyo 101-0047, Japan, tong@kesco.co.jp

**Abstract:** There is great interest in developing all-solid-state lithium-ion batteries. They are ideal micro-power sources for many applications in portable electronic devices, electric vehicles and biomedical engineering. In this work, we present a simulation research based on a two-dimensional model of all-solid-state lithium-ion batteries using COMSOL Multiphysics<sup>®</sup>. The calculation of tertiary current density in the electrolyte and the transport of lithium species in the electrode are coupled. The charge/discharge curves (cell voltage vs. time) for various charge/discharge rates are obtained and analyzed.

**Keywords:** Lithium-ion batteries, All-solid-state, Charge/discharge curves, Numerical simulation.

## 1. Introduction

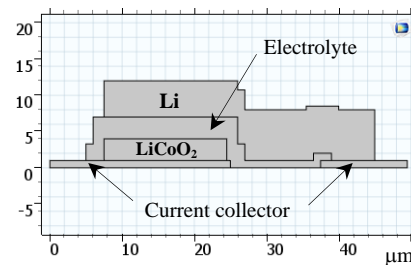
Now all-solid-state lithium-ion batteries have become the state-of-the-art in modern battery technology, which require high energy and power densities, good capacity retention for thousands of discharge/charge cycles, and an extremely low self-discharge rate [1-3]. It is known that all-solid-state lithium-ion batteries are often fabricated by thin film methods, with thicknesses in the range of a few micrometers. Since porous electrodes are not used for this kind of batteries, all electrochemical reactions take place on the interface between the electrolyte and solid electrode domains [4].

Since the conductivity of the solid electrolyte is typically several orders of magnitude lower than that of a traditional liquid electrolyte lithium-ion battery, many previous investigations were focused on material properties of the solid electrolyte. In order to make further improvement in solid-state battery technology, an in-depth understanding of the electrochemical processes involved in the solid-state battery is necessary. There is no doubt that the numerical simulation method is a powerful tool to realize the purpose.

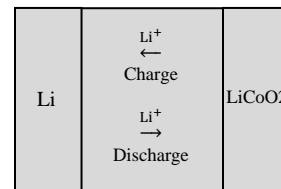
In this work, a two-dimensional model of all-solid-state lithium-ion batteries is developed

based on COMSOL Multiphysics<sup>®</sup>. The tertiary current density in the electrolyte is calculated. The transport of lithium species in the positive electrode is solved in coupling with the calculation of current density. The effects of lithium ions in the electrolyte and of lithium species in the positive electrode on the properties of all-solid-state lithium-ion batteries are obtained and analyzed.

## 2. Numerical Method



(a) Schematic cross section

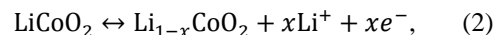


Electrolyte

(b) Transport of  $\text{Li}^+$  in the electrolyte

**Figure 1.** Layout of an all-solid-state lithium-ion battery.

The layout of the all-solid-state lithium-ion battery used in this work is shown in Fig. 1, which has been described in earlier publications [1,5]. The negative electrode comprises metallic lithium and the positive electrode is constructed by the polycrystalline film of  $\text{LiCoO}_2$ . The electrolyte is a solid-state  $\text{Li}_3\text{PO}_4$  film. The electrochemical reactions at the negative and positive electrodes can be represented by



where the reactions shown in eqs. (1) and (2) are described using the Butler-Volmer kinetics

$$i_n = Fk_n \left( \frac{c_{Li^+}}{c_{Li^+,0}} \right)^{\alpha_n} \left( e^{\frac{\alpha_n F \eta}{RT}} + e^{-\frac{(1-\alpha_n)F\eta}{RT}} \right), \quad (3)$$

$$i_p = i_{0,p} \left( e^{\frac{\alpha_p F \eta}{RT}} + e^{-\frac{(1-\alpha_p)F\eta}{RT}} \right), \quad (4)$$

$$i_{0,p} = Fk_p \left( \frac{(c_{Li,max} - c_{Li})c_{Li^+}}{(c_{Li,max} - c_{Li,min})c_{Li^+,0}} \right)^{\alpha_p} \left( \frac{(c_{Li} - c_{Li,min})}{(c_{Li,max} - c_{Li,min})c_{Li^+,min}} \right)^{1-\alpha_p} \quad (5)$$

Here  $F$  is the Faraday's constant,  $k_n$  and  $k_p$  are the rate constants of the reactions (1) and (2), respectively,  $c_{Li^+,0}$  is the total concentration of  $Li^+$  in the electrolyte,  $\alpha_n$  and  $\alpha_p$  are the charge transfer coefficients for the reactions (1) and (2),  $c_{Li,max}$  and  $c_{Li,min}$  are the maximum and minimum levels of lithium species in the positive electrode,  $R$  is the gas constant, and  $T$  is the temperature.

In charge process, the oxidation reactions at the surface of  $LiCoO_2$  occur and the produced  $Li^+$  ions move to the negative electrode,  $Li$ , as shown in Fig. 1(b). On the contrary, for discharge process, the reduction reactions at the surface of  $LiCoO_2$  occur and  $Li^+$  ions obtained from the negative electrode come to  $LiCoO_2$  and consumed at the surface of  $LiCoO_2$ . The chemical reaction in the electrolyte



describes the ionization reaction, where the immobile oxygen-binding lithium  $Li^0$  is transferred to  $Li^+$  and  $n^-$ . The transport of  $Li^+$  and  $n^-$  is solved by the Nernst-Planck equation

$$\mathbf{N}_i = -D_i \nabla c_i + \frac{z_i F}{RT} D_i c_i \nabla \phi_i, \quad (7)$$

where  $c_i$  and  $D_i$  are the concentration and diffusion coefficient of species, respectively,  $z_i$  is the charge of species, and  $\phi_i$  is the electrolyte potential.

The positive electrode consists of trivalent cobalt oxide species, in which the lithium ions are intercalated.  $Li^+$  ions in  $LiCoO_2$  are screened by the mobile electrons, which accompany  $Li^+$  when they move from one interstitial site to the other. The mass transport of lithium ions inside the positive electrode can be described by the standard diffusion equation [4]. In this work, the transport of lithium species in the positive electrode is described by the Fick's law

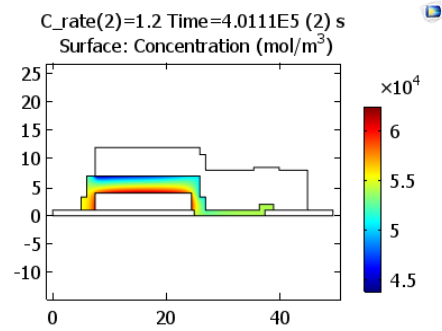
$$\mathbf{N}_{Li} = -D_{Li} \nabla c_{Li}. \quad (8)$$

where  $c_{Li}$  and  $D_{Li}$  are the concentration and diffusion coefficient of lithium species, respectively. In calculations, the negative electrode domain is not involved. The calculation of tertiary current density is carried out in the electrolyte and the solution of the transport of lithium species is performed in the positive electrode.

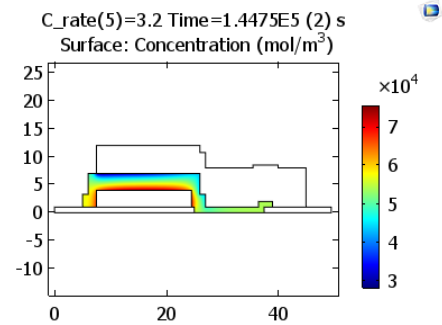
### 3. Simulation results

#### 3.1 Charge characteristics

Figures 2-5 show the calculated results of charge process of the all-solid-state lithium-ion battery. The battery is charged up to 4.2 V. The charge rates are 0.8, 1.2, 1.6, 2.4, and 3.2 C. Results show that the concentration deviation from the equilibrium concentration in the electrolyte is higher for higher charge rates. Figure 2 shows the concentrations of lithium ion in the electrolyte at the end of 1.2 and 3.2 C-rate charge. At the charge rate of 3.2 C, the maximum and minimum concentrations of lithium ion have arrived at  $7.6 \times 10^4$  mol/m<sup>3</sup> and



(a) C-rate = 1.2



(b) C-rate = 3.2

**Figure 2.** Concentrations of lithium ions in the electrolyte at the end of charge.

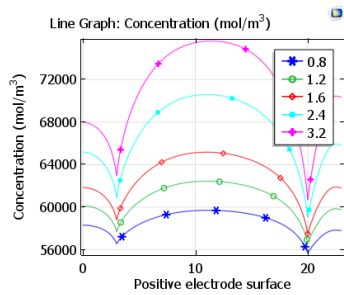
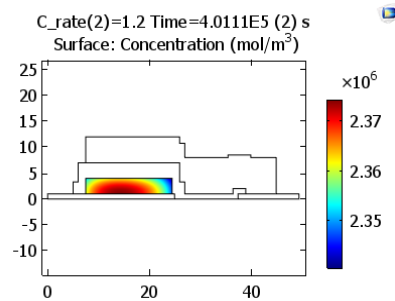
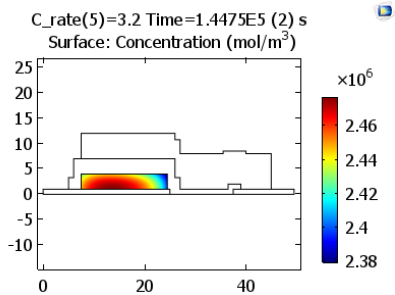


**Figure 3.** Concentrations of lithium ions on the surface of positive electrode at the end of charge for various charge rates.



(a) C-rate = 1.2



(b) C-rate = 3.2

**Figure 4.** Concentrations of lithium species in the positive electrode at the end of charge.

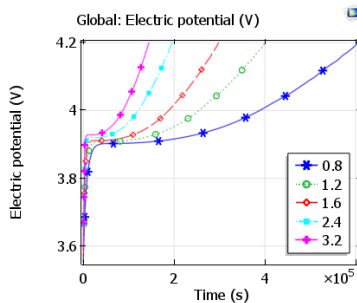
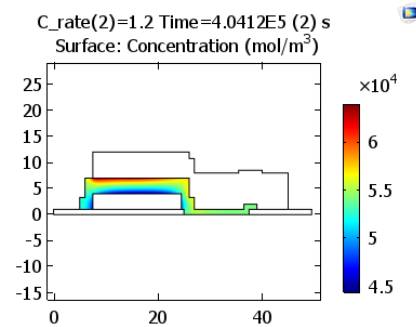


**Figure 5.** Charge curves (cell voltage vs. time) for various charge rates.

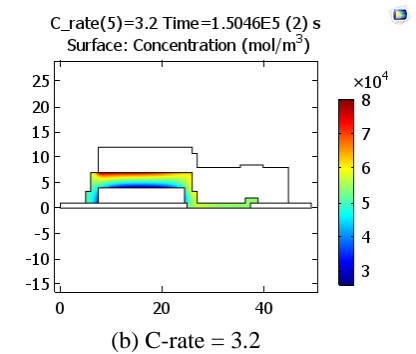
$2.8 \times 10^4 \text{ mol/m}^3$  largely deviated from the initial value of  $5.4 \times 10^4 \text{ mol/m}^3$ . The oxidation reactions at the surface of positive electrode cause high concentration distribution of  $\text{Li}^+$  ions in the neighborhood of positive electrode. The concentrations of  $\text{Li}^+$  ions on the surface of positive electrode at the end of charge for various charge rates are shown in Fig. 3. In the positive electrode, due to the same reactions at the surface, the concentration of lithium species close to the electrode surface becomes low, as shown in Fig. 4. The charge curves (cell voltage vs. time) for the different charge rates are given in Fig. 5. The cell voltage by charge has a steep rise until about 3.9 V and then spreads around corresponding to the different charge rates.

### 3.2 Discharge characteristics

It is shown that the concentration deviation from the equilibrium concentration in the electrolyte is similar to that of charge process, as shown in Fig. 6. However, for discharge process, the chemical reactions occurred at the surface of positive electrode are reduction reactions, which cause low concentration distribution of  $\text{Li}^+$  ions



(a) C-rate = 1.2



(b) C-rate = 3.2

**Figure 6.** Concentrations of lithium ions in the electrolyte at the end of discharge.

in the neighborhood of positive electrode. The concentrations of  $\text{Li}^+$  ions on the surface of positive electrode at the end of discharge for various discharge rates are shown in Fig. 7. In the positive electrode, the reduction reactions at the surface cause the concentration of lithium species close to the electrode surface to be high, as shown in Fig. 8. The discharge curves for the different discharge rates are given in Fig. 9. The cell voltage before depletion is shifted downwards for higher discharge rates. This could be deduced by a fact that for higher currents, the internal losses increase.

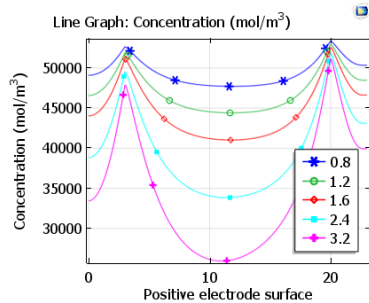


**Figure 7.** Concentrations of lithium ions on the surface of positive electrode at the end of discharge for various discharge rates.

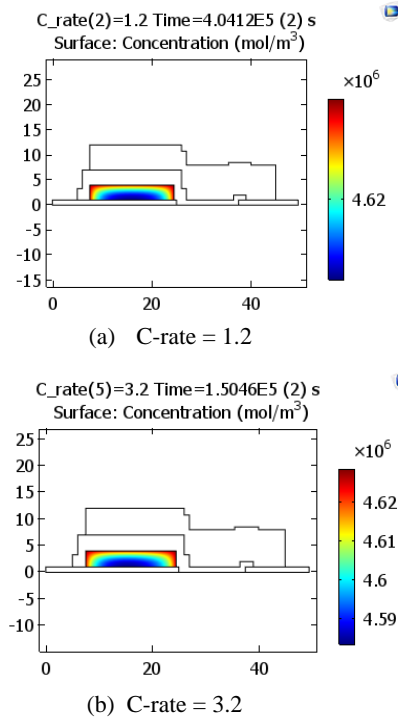


**Figure 8.** Concentrations of lithium species in the positive electrode at the end of discharge.

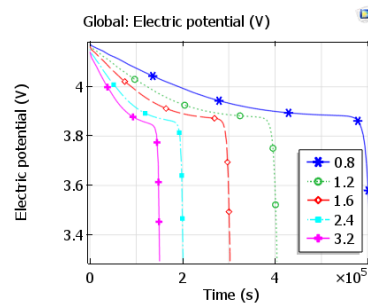


**Figure 9.** Discharge curves (cell voltage vs. time) for various discharge rates.

## 4. Conclusions

This paper reports the simulation results of an all-solid-state lithium-ion battery. The variations of the concentrations of  $\text{Li}^+$  ions in the electrolyte and of lithium species in the positive electrode are presented. It is found that the battery can be quickly charged at the initial stage of charge process, but it has a smooth discharge before depletion for the different charge/discharge rates. It could be concluded that the developed model would be beneficial in realizing industrial applications of all-solid-state lithium-ion batteries in near future.

## 5. References

1. N. J. Dudney, "Solid-state thin-film rechargeable batteries", *Materials Science and Engineering B* **116**, 245-249 (2005).
2. A. Patil, V. Patil, D. W. Shin, J. W. Choi, D. S. Paik, and S. J. Yoon, "Issue and challenges facing rechargeable thin film lithium batteries", *Materials Research Bulletin* **43**, 1913-1942 (2008).
3. J. P. Carmo, R. P. Rocha, A. F. Silva, L. M. Goncalves, and J. H. Correia, "A thin-film rechargeable battery for integration in stand-alone microsystems", *Procedia Chemistry* **1**, 453-456 (2009).
4. D. Danilov, R. A. H. Niessen, and P. H. L. Notten, "Modeling all-solid-state Li-ion batteries", *Journal of The Electrochemical Society* **158** (3), A215-A222 (2011).
5. J. B. Bates, N. J. Dudney, B. Neudecker, A. Ueda, and C. D. Evans, "Thin-film lithium and lithium-ion batteries", *Solid State Ionics* **135**, 33-45 (2000).